

# Dielectric anisotropy in liquid crystal mixtures with nematic and smectic phases

Xing-Zhou Tang(汤星舟)<sup>1,†</sup>, Jia-Yao Ye(叶家耀)<sup>1,‡</sup>, Zi-Ye Wang(王子烨)<sup>1</sup>, Hao-Yi Jiang(姜皓译)<sup>1</sup>,  
Xiao-Hu Shang(尚小虎)<sup>1</sup>, Zhao-Yan Yang(杨朝雁)<sup>1,‡</sup>, and Bing-Xiang Li(李炳祥)<sup>1,2,§</sup>

<sup>1</sup>Nanjing University of Posts and Telecommunications, College of Electronic and Optical Engineering & College of Flexible Electronics (Future Technology), Nanjing 210023, China

<sup>2</sup>National Laboratory of Solid State Microstructures, College of Engineering and Applied Sciences, Nanjing University, Nanjing 210023, China

(Received 11 March 2024; revised manuscript received 29 April 2024; accepted manuscript online 17 May 2024)

The modulation of dielectric anisotropy ( $\Delta\epsilon$ ) is pivotal for elucidating molecular interactions and directing the alignment of liquid crystals. In this study, we combine liquid crystals with opposing dielectric anisotropies to explore the impact of varying concentrations on their properties. We report the sign-reversal of  $\Delta\epsilon$  in both the nematic and smectic A phases of these mixed liquid crystals, alongside a dual-frequency behaviour across a broad temperature spectrum. Our research further quantifies the influence of mixture ratios under various temperatures and electric field frequencies. This exploration may pave the way for the discovery of new physical phenomena.

**Keywords:** mixed liquid crystal, dielectric anisotropy, tunable, nematic, smectic

**PACS:** 77.84.Nh

**DOI:** 10.1088/1674-1056/ad4cd7

## 1. Introduction

Liquid crystals (LCs) are versatile soft materials that occupy the intermediate state between solid and liquid, characterized by their anisotropic properties. The inherent anisotropy of LCs has led to their widespread application in various fields, including display technology,<sup>[1-3]</sup> optical switches,<sup>[4,5]</sup> light modulators,<sup>[6,7]</sup> and beam splitters.<sup>[8]</sup> The collective orientation of LC molecules, known as the director, plays a crucial role in their behavior. LCs are classified into different phases based on molecular order, with nematic and smectic phases being most common. Molecules in nematic phase have orientational order while having both orientational order and partial positional order during smectic phase.<sup>[9,10]</sup> The orientational order leads to optical anisotropy, expressed as  $\Delta n = n_e - n_o$ , and dielectric anisotropy, denoted as  $\Delta\epsilon = \epsilon_{\parallel} - \epsilon_{\perp}$ , where  $n_e$  and  $n_o$  are the extraordinary and ordinary refractive indices, and  $\epsilon_{\parallel}$  and  $\epsilon_{\perp}$  are the dielectric permittivities parallel and perpendicular to the director. Research into the dielectric anisotropy of LCs provides insights into intermolecular interactions and molecular orientation within LCs.

Significant attention has been given to the dielectric anisotropy of LCs,<sup>[11-16]</sup> with a particular focus on dual-frequency LCs (DFLCs),<sup>[17-24]</sup> which exhibit frequency-dependent dielectric anisotropy and are used in rapid-response electro-optic controls, optoelectronic devices, and displays. The crossover frequency ( $f_c$ ) is a critical parameter in DFLCs that determines the sign of  $\Delta\epsilon$ , being positive when the electric field frequency is below  $f_c$  and negative when above.<sup>[25]</sup>

Previous studies on DFLCs have primarily focused on the nematic phase<sup>[14,26]</sup> and interesting works have been conducted in cholesteric liquid by Lee *et al.*<sup>[27]</sup> However, recent observations by Kosuke Kaneko *et al.*<sup>[28]</sup> revealed dual-frequency characteristics in the smectic A phase over a wide temperature range in a mixed LC system. Despite this advancement, a systematic investigation of dual-frequency mixed LCs with varying ratios has not been conducted. Our work aims to address this gap by presenting detailed observations of dielectric anisotropy across different phases and compiling these findings into a phase diagram. Earlier attempts to reverse the sign of dielectric anisotropy involved incorporating side-chain polymers,<sup>[29]</sup> quantum dots,<sup>[30]</sup> and dyes<sup>[31]</sup> into LCs or altering the temperature,<sup>[32]</sup> but these methods were limited by high crossover frequencies and narrow tunable ranges. Our study overcomes these challenges by achieving a broad tunable range of  $\Delta\epsilon$  and crossover frequencies.

In this work, we prepare a series of mixed LC samples with both positive and negative  $\Delta\epsilon$  in different proportions. We present the phase diagram and establish the relationship between the phase transition temperature and concentration. We investigate the effects of electric field frequency, temperature, and weight ratios of different LCs on the dielectric anisotropy of the mixtures. We explore the relationship between  $\Delta\epsilon$  and temperature in the nematic phase and observe dual-frequency phenomena in the smectic A phase. Finally, by varying the frequency, we summarize the minimum and maximum values of dielectric anisotropy at different temperatures

<sup>†</sup>These authors contributed equally to this work.

<sup>‡</sup>Corresponding author. E-mail: zyyang@njupt.edu.cn

<sup>§</sup>Corresponding author. E-mail: bxli@njupt.edu.cn

for each mixture. This work lays the foundation for addressing specific physical problems and has potential applications in the field of electro-optic modulation.

## 2. Experimental details

In this study, we produced a series of mixed liquid crystal (LC) samples by combining two types of LCs: 4'-Octyl-4-biphenylcarbonitrile (8CB, acquired from Jiangsu Hecheng Display Technology Co., Ltd) and 4'-butyl-4-heptylbicyclohexyl-4-carbonitrile (CCN47, sourced from Nematel GmbH, Germany) in varying ratios. The molecular structures of these compounds are depicted in Fig. 1. The CCN47 molecule, characterized by its transverse dipole moment, exhibits negative dielectric anisotropy, whereas the longitudinal dipole moment in the 8CB molecule results in a positive dielectric anisotropy ( $\Delta\epsilon > 0$ ). For instance, CCN47 demonstrates a dielectric anisotropy of  $\Delta\epsilon = -5.1$  at a frequency of 1 kHz and an optical anisotropy of  $\Delta n = 0.029$  when illuminated at a wavelength of 589 nm at 40 °C. In contrast, 8CB shows  $\Delta\epsilon = 7.5$  and  $\Delta n = 0.133$  under the same conditions at 25 °C. Both materials transition through nematic and smectic A phases and have molar masses of 345 g/mol for CCN47 and 291 g/mol for 8CB, respectively.

To prepare the mixtures, we combined CCN47 and 8CB in designated ratios, transferred them into reagent bottles, and subjected the solutions to ultrasonic agitation for 20 min to ensure thorough mixing. Subsequently, the mixtures were heated on a hotplate at 60 °C for five hours to achieve homogeneity. The components in the mixtures are denoted as  $C_i$ , where  $i$  represents the mass percentage of CCN47 (e.g.,  $C_{20}$  indicates a mass ratio of CCN47 to 8CB of 2:8). We explored 11 distinct combinations, incrementing the CCN47 content from 0% to 100% in 10% intervals.

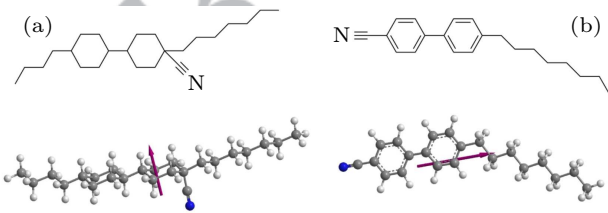


**Fig. 1.** Molecular structures of (a) CCN47 and (b) 8CB. Arrows indicate the direction of permanent dipoles.

Liquid crystal (LC) cells were constructed using two glass plates equipped with transparent indium tin oxide (ITO) electrodes. To assess the dielectric constants  $\epsilon_{\parallel}$  and  $\epsilon_{\perp}$  of the mixtures, we prepared two types of LC cells. One type, designed for the measurement of  $\epsilon_{\perp}$ , utilized a parallel-aligned LC cell. The glass substrates were coated with polyimide 4220 (from Nanjing Ningcui Optical Technology Co., Ltd.) as the parallel orientation agent. This agent was spin-coated at 2500 rpm for 25 s, pre-dried at 130 °C for 2 min, and cured at 230 °C

for 20 min. Post-curing, the agent was unidirectionally rubbed to achieve the initial parallel orientation. The second type, for measuring  $\epsilon_{\parallel}$ , used a vertically-aligned LC cell, with polyamic acid 4070 (also from Nanjing Ningcui Optical Technology Co., Ltd.) as the vertical orientation agent. The process involved spin-coating at 2500 rpm for 25 s, pre-drying at 80 °C for 5 min, and curing at 210 °C for 60 min. To attain the desired LC cell thickness, UV glue containing silicon particles was applied to the glass slides. The LC cell thickness was maintained within 7  $\mu\text{m}$ –11  $\mu\text{m}$ .

In our experiments, the ITO-coated cell functioned as a capacitor. The capacitance value, influenced by the dielectric permittivity of the LC, the electrode area ( $S$ ), and the LC cell thickness ( $d$ ), was defined by the following equation:

$$C = \epsilon \frac{S}{d}. \quad (1)$$

Subsequently, the relative dielectric permittivity of each mixture ( $\epsilon_r$ ) was computed from the capacitance values

$$\epsilon_r = \frac{\epsilon}{\epsilon_{\text{empty}}} = \frac{C_{\text{filled}}d/S}{C_{\text{empty}}d/S} = \frac{C_{\text{filled}}}{C_{\text{empty}}}. \quad (2)$$

Here,  $\epsilon_{\text{empty}}$  approximates the permittivity of an empty cell,  $C_{\text{filled}}$  is the capacitance of a cell filled with the mixed LCs, and  $C_{\text{empty}}$  is the capacitance of the empty cell.

The contribution of dielectric energy is given by<sup>[33]</sup>

$$f_{\text{diel}} = -\frac{1}{2}\epsilon_0\epsilon_{ij}E_iE_j, \quad (3)$$

where  $\epsilon_0$  relates to the vacuum dielectric permittivity, and  $\epsilon_{ij}$  corresponds to the tensorial dielectric permittivity of the nematic material and can be expressed as

$$\epsilon_{ij} = \epsilon_{\perp}\delta_{ij} + (\epsilon_{\parallel} - \epsilon_{\perp})n_in_j, \quad (4)$$

where  $n_i$  and  $n_j$  correspond to the components of the director field.

To measure the dielectric permittivity in perpendicular ( $\epsilon_{\perp}$ ) and parallel ( $\epsilon_{\parallel}$ ) directions, the mixed LCs were injected into the respective oriented cells during the isotropic phase before being quenched to the nematic phase. Capacitance measurements for  $C_{\text{filled}}$  and  $C_{\text{empty}}$  were taken with an LCR meter (4284A, Hewlett-Packard), which output a sine wave signal at 0.2 V · rms across a frequency range of 20 Hz to 1 MHz. Dielectric permittivity was tested over a temperature range from  $-40$  °C to 70 °C, with cooling at the rate of 2 °C/min.

The phase transition temperatures were determined by first heating the mixtures to the isotropic phase, then cooling at a rate of 2 °C/min, recording the temperatures at which the phase transition completed. Observations were made using a polarizing microscope (Nikon ECLIPSE Ci-POL) in an LC cell with parallel orientation. In the isotropic phase and

when aligned parallel to the microscope polarizer, the LCs appeared black in the field of view. For optimal observation, the cell's rubbing direction was perpendicular to the polarizer direction. Temperature control for the samples was maintained using a hot plate (HCS402, Instec) and a temperature controller (mK2000B, Instec).

### 3. Results and discussion

To map the phase diagram of mixed liquid crystals, POM textures of 11 samples with varying CCN47 to 8CB ratios were observed over a temperature range of  $-40\text{ }^{\circ}\text{C}$  to  $70\text{ }^{\circ}\text{C}$ , as presented in Fig. 2(a). Distinct phases were evident among the different samples.  $C_{30}$ ,  $C_{40}$ ,  $C_{50}$ , and  $C_{60}$  exhibited the isotropic phase at higher temperatures and maintained the nematic phase down to  $-40\text{ }^{\circ}\text{C}$ .  $C_{20}$  and  $C_{70}$  transitioned from

isotropic to nematic and then to the crystalline phase. The  $C_{100}$ ,  $C_{90}$ ,  $C_{80}$ ,  $C_{10}$ , and  $C_0$  samples shifted from isotropic to nematic, smectic A, and eventually to crystalline. Moreover, the isotropic-to-nematic transition temperature ( $T_{NI}$ ) was dependent on the CCN47 content;  $T_{NI}$  dropped from  $40.5\text{ }^{\circ}\text{C}$  to  $28\text{ }^{\circ}\text{C}$  as CCN47 increased from 0% ( $C_0$ ) to 30% ( $C_{30}$ ) and rose again with further CCN47 increase, reaching about  $59\text{ }^{\circ}\text{C}$  for  $C_{100}$ . Silica particles were added to the LCs to differentiate the phases, and POM images of  $C_{10}$  showed as in Fig. 2(b) revealed distinct phase characteristics. In the isotropic phase, a uniform black appearance was noted, while color variations in the nematic phase correlated to LC molecular alignment. In the smectic A phase, layer-like structures were observed, and diverse textures appeared in the crystalline phase, with differences becoming more pronounced after adding a full-wave plate.

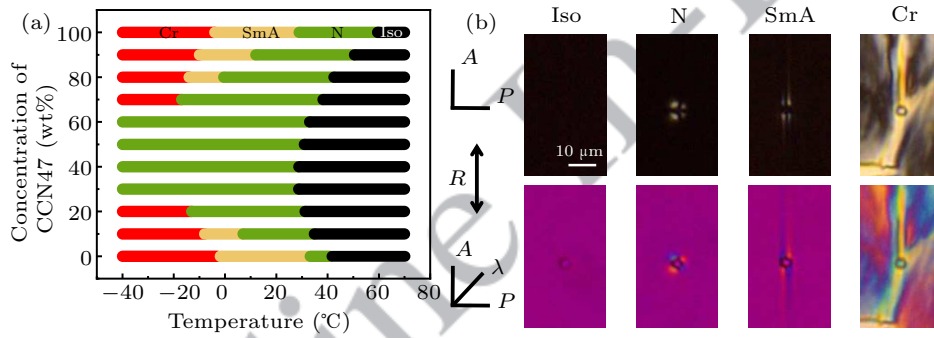


**Fig. 2.** (a) The phase diagram of various mixtures. Cr, SmA, N, and Iso represent the crystalline phase, smectic A phase, nematic phase, and isotropic phase, respectively. (b) POM images of  $C_{10}$  in isotropic, nematic, smectic A, and crystalline phases under crossed polarizers without and with a full-wave plate. The rubbing direction  $R$  is indicated by the double arrows.

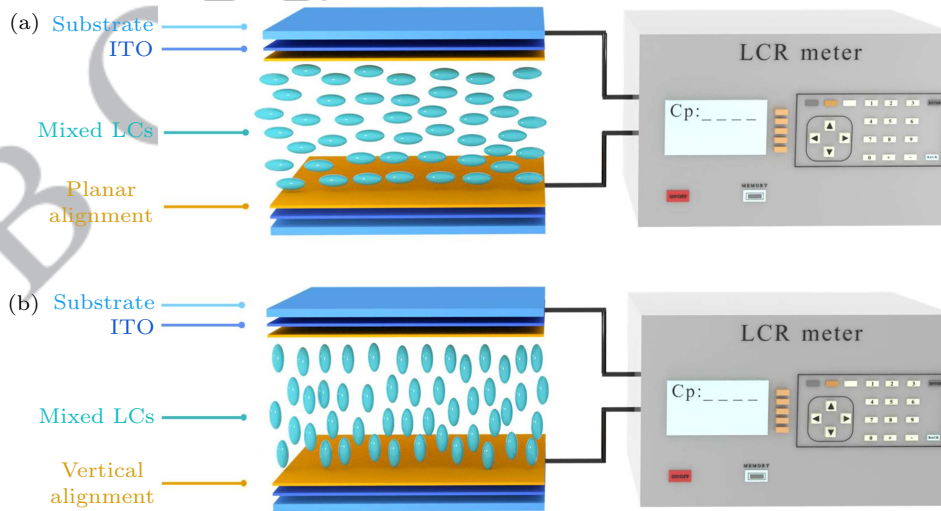


**Fig. 3.** The principle schematics of dielectric permittivity verifying with frequency. (a) Measurement of  $C_{\text{filled}}$  for  $\epsilon_{\perp}$ . (b) measurement of  $C_{\text{filled}}$  for  $\epsilon_{\parallel}$ .

Dielectric permittivity in the perpendicular ( $\epsilon_{\perp}$ ) and parallel ( $\epsilon_{\parallel}$ ) directions was recorded across different frequencies. An LCR meter is used to measure capacitances of liquid crystal cells as shown in Fig. 3, and the frequency of applied voltage from LCR meter is controlled by a Labview program. Figure 4 highlights five key observations from the ex-

perimental study: the dielectric anisotropy of the nematic liquid crystal mixtures remained positive (Fig. 4(a)), approached zero (Fig. 4(b)), remained negative (Fig. 4(c)), exhibited dual-frequency characteristics in the nematic mixture (Fig. 4(d)), and exhibited dual-frequency characteristics in the smectic phase mixture (Fig. 4(e)). As illustrated in Fig. 4(a),  $\epsilon_{\perp}$  of

$C_{20}$  remained stable while  $\epsilon_{\parallel}$  diminished from 13 to 8.5 at higher frequencies, indicating a positive dielectric anisotropy at 20 °C, as shown in Fig. 4(f).  $C_{70}$ 's  $\epsilon_{\parallel}$  and  $\epsilon_{\perp}$  at this temperature were nearly identical, leading to a dielectric anisotropy of zero (Fig. 4(f)). For  $C_{80}$ , both  $\epsilon_{\parallel}$  and  $\epsilon_{\perp}$  stayed constant up to  $10^5$  Hz and decreased at higher frequencies, with  $\epsilon_{\parallel}$  consistently below  $\epsilon_{\perp}$ , resulting in negative dielectric anisotropy (Fig. 4(f)). These findings demonstrate that increasing CCN47 content adjusts dielectric anisotropy from positive to negative at a consistent temperature. When  $C_{20}$  was reexamined after cooling, a decline in both  $\epsilon_{\parallel}$  and  $\epsilon_{\perp}$  was noted at elevated

frequencies (Fig. 4(d)). Unlike its behavior at higher temperatures,  $C_{20}$  at  $-10$  °C showed  $\epsilon_{\parallel}$  lower than  $\epsilon_{\perp}$  past  $2 \times 10^5$  Hz, indicative of dual-frequency behavior (Fig. 4(f)). Notably,  $C_{10}$  also displayed dual-frequency characteristics at  $-6$  °C in the smectic A phase (Figs. 4(e) and 4(f)). The dielectric permittivity of the mixtures at 0 °C, 10 °C, and 20 °C were presented in the supplementary file (see Figs. S1–S3 in supporting information). Additionally, the dielectric permittivity of pure 8CB and CCN47 in crystalline, smectic A, nematic, and isotropic phases were shown in Fig. S4.

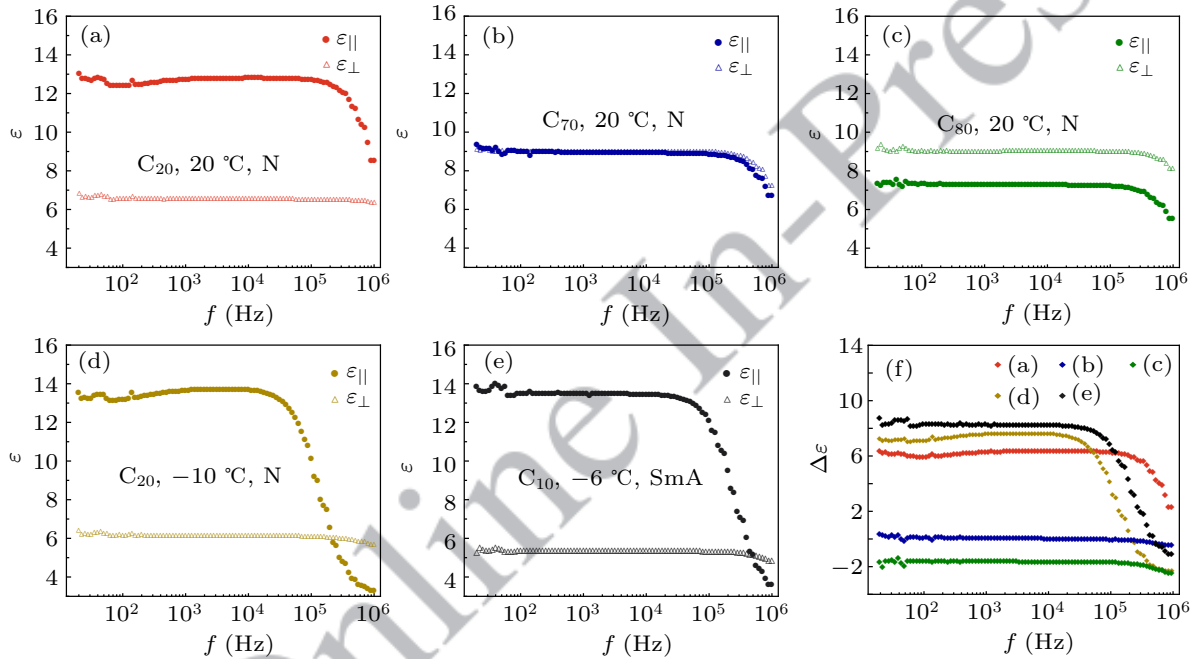


**Fig. 4.** The dielectric permittivity  $\epsilon_{\parallel}$  and  $\epsilon_{\perp}$  of (a)  $C_{20}$  in 20 °C, (b)  $C_{70}$  in 20 °C, (c)  $C_{80}$  in 20 °C, (d)  $C_{20}$  in  $-10$  °C and (e)  $C_{10}$  in  $-6$  °C, (f)  $\Delta\epsilon$  corresponding to panels (a)–(e).

Furthermore, we investigated the relationship between the dielectric permittivity of the mixtures and temperature. As the temperature increased, the mixtures exhibited three outcomes: dielectric anisotropy remained positive, dual-frequency characteristics were observed, and dielectric anisotropy remained negative. Both  $\epsilon_{\perp}$  and  $\epsilon_{\parallel}$  fluctuated with temperature within each mixture, correspondingly impacting the dielectric anisotropy,  $\Delta\epsilon$ . The main results are presented in Fig. 5, while the results for the other eight mixtures are provided in Fig. S5 of supporting information. As illustrated in Fig. 5(a), the  $\Delta\epsilon$  of  $C_{20}$  is null within the temperature ranges corresponding to the crystalline and isotropic phases. However, upon entering the nematic phase domain,  $\epsilon_{\parallel}$  and  $\epsilon_{\perp}$  of  $C_{20}$  increase sharply, with the final  $\epsilon_{\parallel}$  exceeding  $\epsilon_{\perp}$ , denoting a positive dielectric anisotropy in the nematic phase. In contrast, the  $\Delta\epsilon$  of  $C_{60}$  undergoes distinct transformations, shifting from negative to positive within the nematic phase's temperature range, as evidenced in Fig. 5(b), where the transition occurs around  $-20$  °C.  $\Delta\epsilon$  of  $C_{60}$  remains neutral within the isotropic phase temperature range. Figure 5(c) delineates the variation of  $\epsilon_{\perp}$ ,

$\epsilon_{\parallel}$ , and  $\Delta\epsilon$  with temperature for  $C_{90}$ , showcasing a consistently negative  $\Delta\epsilon$  in both the smectic A and nematic phases. The extremities of  $\Delta\epsilon$  for each sample were computed across a temperature spectrum of 60 °C to  $-40$  °C, and the outcomes are displayed in Fig. 5(d). At a fixed frequency of 20 kHz, samples like  $C_0$ ,  $C_{10}$ , and  $C_{20}$  manifest a positive  $\Delta\epsilon$ , whereas  $C_{70}$ ,  $C_{80}$ ,  $C_{90}$ , and  $C_{100}$  exhibit a negative  $\Delta\epsilon$ . An inverse  $\Delta\epsilon$  is observed in  $C_{30}$ ,  $C_{40}$ ,  $C_{50}$ , and  $C_{60}$ . These observations unequivocally establish that the dielectric anisotropy in mixed liquid crystals is temperature-dependent, facilitating the manifestation of inverse  $\Delta\epsilon$  within the same sample.

The correlation between the crossover frequency and temperature is traditionally described by the following Arrhenius equation<sup>[34]</sup>

$$f_c = A \exp(-E/kT). \quad (5)$$

In this equation,  $A$  denotes a material constant,  $E$  the activation energy,  $k$  the Boltzmann constant, and  $T$  the temperature. This relationship suggests that the crossover frequency

increases with rising temperature. We explored this correlation in samples C<sub>10</sub> through C<sub>60</sub>, as illustrated in Fig. S6. The natural logarithm of the crossover frequency for these LC mixtures with fixed proportions exhibited a linear dependence on temperature, as depicted in Figs. S6(a)–S6(f). The dielectric relaxation properties of 8CB are presented in Table S1. The relaxation frequency of 8CB decreased with decreasing temperature, remaining above 1 MHz at room temperature. The crossover frequency of a dual-frequency mixture primarily relies on the relaxation frequency of the molecular S-mode of the dielectrically positive component. Consequently, in this study, the crossover frequency of the mixtures was close to 1 MHz below room temperature (e.g., C<sub>60</sub>,  $f_c = 860$  kHz at 20 °C; C<sub>10</sub>,  $f_c = 768$  kHz at 0 °C).

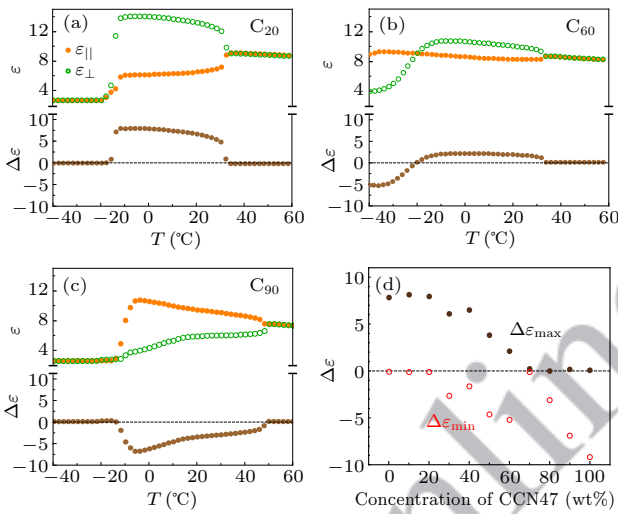


**Fig. 5.** The change of dielectric permittivity and dielectric anisotropy from 60 °C to -40 °C in (a) C<sub>20</sub>, (b) C<sub>60</sub>, and (c) C<sub>90</sub>. (d) The maximum and minimum of  $\Delta\epsilon$  in different mixtures. All the frequency of output signal is fixed on 20 kHz.

The interplay between dielectric anisotropy and the CCN47 concentration in the mixtures at a fixed frequency and temperature was also scrutinized, as shown in Fig. 6(a). At a temperature of 5 °C below the  $T_{NI}$  and a frequency of 20 kHz,  $\Delta\epsilon$  was observed to decrease linearly with rising CCN47 concentration in the LC mixtures, following the linear relationship<sup>[35]</sup>

$$\Delta\epsilon_{\text{mix}} = \sum c_i \Delta\epsilon_i. \quad (6)$$

Here,  $\Delta\epsilon_{\text{mix}}$  is derived from the dielectric anisotropy of the constituents,  $\Delta\epsilon_i$ , and their molar fractions,  $c_i$ . We further explored the maxima and minima of  $\Delta\epsilon$  in LC mixtures at different frequencies (Figs. 6(b)–6(d)), with the temperature set 10 °C, 20 °C, and 30 °C below the  $T_{NI}$ , respectively. It was found that the maximum  $\Delta\epsilon$  slightly rose and the minimum progressively declined as the temperature decreased. Additionally, the range of mixtures demonstrating dual-frequency properties expanded during the cooling process.

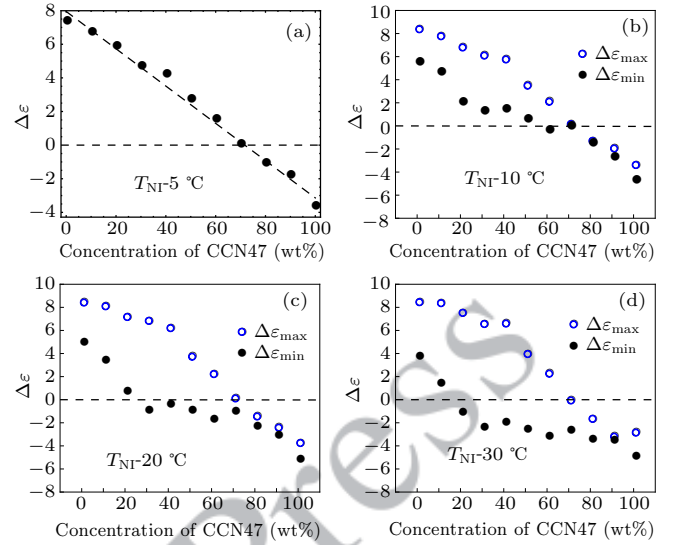


**Fig. 6.** (a) The relationship between dielectric anisotropy and the concentration of CCN47 at the frequency of 20 kHz and the temperature of 5 °C below  $T_{NI}$ .  $\Delta\epsilon$  of the mixtures with different concentrations of CCN47 at the temperature of (b) 10 °C, (c) 20 °C, and (d) 30 °C below  $T_{NI}$ , and the frequency is varied from 20 Hz to 1 MHz.

Figure 7(a) details the temperature scope exhibiting dual-frequency characteristics under frequencies ranging from 20 Hz to 1 MHz for mixed LCs with the CCN47 concentration range of 10 wt%–60 wt%. The data indicate an expanding temperature range for dual-frequency behavior with higher CCN47 concentrations, extending to about 60 °C at 60-wt% CCN47. Notably, the dual-frequency range was consistent within the nematic phase for CCN47 concentrations of 20 wt% to 60 wt%, while at 10 wt% CCN47, the smectic A phase was observed. This indicates dual-frequency occurrence in both nematic and smectic A phases, underscoring the unique electro-optical properties within these concentration brackets. Figure 7(b) compiles the minimum and maximum  $\Delta\epsilon$  for each sample across varied temperatures. Measurements were confined to frequencies above 1 kHz to mitigate data fluctuation at lower frequencies. Positive and negative  $\Delta\epsilon$  values are represented by red and blue, respectively, with the color intensity correlating to the magnitude of  $\Delta\epsilon$ . Neutrality,  $\Delta\epsilon = 0$ , is denoted in white. At a fixed temperature, if both the minimum and maximum values are positive (indicated by the red color), the mixture exhibits positive dielectric anisotropy at that temperature. Conversely, if both the minimum and maximum values are negative (indicated by the blue color), the mixture exhibits negative dielectric anisotropy. The mixture exhibits dual-frequency characteristics when the signs of the minimum and maximum values are inconsistent, with the minimum value being negative (blue) and the maximum value being positive (red). These results elucidate the temperature at which  $\Delta\epsilon$  inversion occurs and the relative magnitude of  $\Delta\epsilon$  within the CCN47 concentration range of 10 wt%–60 wt%. Moreover, as the isotropic phase of LCs is characterized by a null  $\Delta\epsilon$ ,  $T_{NI}$  for the different mixtures is also reflected in Fig. 7(b).

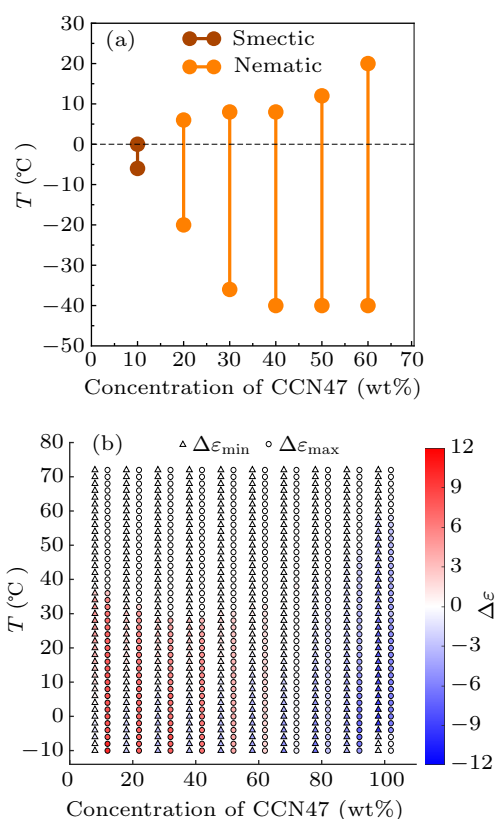


**Fig. 7.** (a) The temperature range of dual-frequency characteristics for the LCs mixtures with different mass ratios of CCN47. (b) The minimum and maximum of  $\Delta\varepsilon$  in mixtures with different mass ratios of CCN47 at different temperatures. Red represents  $\Delta\varepsilon > 0$ , white represents  $\Delta\varepsilon = 0$ , and blue represents  $\Delta\varepsilon < 0$ .

## 4. Conclusions

In summary, our study systematically investigates a series of liquid crystal compounds by combining the positive dielectric anisotropy liquid crystal 8CB with the negative dielectric anisotropy liquid crystal CCN47 in different mass ratios. The nematic phase is consistently observed across all mixtures, with the smectic A phase appearing in specific ratios, notably  $C_{10}$ ,  $C_{80}$ , and  $C_{90}$ . By adjusting the frequency of the applied AC field, dual-frequency behavior is achieved in six mixtures:  $C_{10}$  in the smectic A phase and  $C_{20}$  through  $C_{60}$  in the nematic phase. Moreover, our research demonstrates the ability to toggle between positive and negative dielectric anisotropy by varying the temperature or the CCN47 ratio. We also document a linear relationship between the natural logarithm of crossover frequency and temperature, and a linear decrease in dielectric anisotropy with increasing CCN47 concentration. Our findings may lay the groundwork for advancements in ultrafast electro-optic regulation and phase modulation technologies.

## Acknowledgements

Project supported by the National Key Research and Development Program of China (Grant No. 2022YFA1405000),

the National Natural Science Foundation of China (Grant No. 62375141), the Natural Science Foundation of Jiangsu Province, Major Project (Grant No. BK20212004), and the Natural Science Research Start-up Foundation of Recruiting Talents of Nanjing University of Posts and Telecommunications (Grant Nos. NY222122 and NY222105).

## References

- [1] Ma L L, Li C Y, Pan J T, Ji Y E, Jiang C, Zheng R, Wang Z Y, Wang Y, Li B X and Lu Y Q 2022 *Light. Sci. Appl.* **11** 270
- [2] Lu Y Q and Li Y 2021 *Light. Sci. Appl.* **10** 122
- [3] Yang D K and Wu S T 2014 *Fundamentals of liquid crystal devices* (Chichester: John Wiley & Sons) pp. 199-200
- [4] Huh J W, Oh S W, Seo J H and Yoon T H 2021 *J. Mol. Liq.* **327** 114846
- [5] Wyatt P J, Bailey J, Nagaraj M and Jones J C 2021 *Nat. Commun.* **12** 4717
- [6] Sun J, Chen Y and Wu S T 2012 *Opt. Express* **20** 20124
- [7] Yin K, Hsiang E L, Zou J, Li Y N, Yang Z Y, Yang Q, Lai P C, Lin C H and Wu S T 2022 *Light. Sci. Appl.* **11** 161
- [8] Mur U, Ravnik M and Seč D 2022 *Sci. Rep.* **12** 1
- [9] Ericksen J L 1966 *Arch. Ration. Mech. Anal.* **4** 231
- [10] Leslie F M 1966 *Q. J. Mech. Appl. Math.* **19** 357
- [11] Ayeb H, Derbali M, Mouhli A, Soltani T, Jomni F, Fresnais J and Lacaze E 2020 *Phys. Rev. E* **102** 052703
- [12] Missaoui T, Amor I B, Soltani T, Ouada H B, Jeanneau E and Chevalier Y 2020 *J. Mol. Liq.* **304** 112726
- [13] Trbojevic N, Read D J and Nagaraj M 2017 *Phys. Rev. E* **96** 052703
- [14] Mrukiewicz M, Perkowski P and Garbat K 2015 *Liq. Cryst.* **42** 1036
- [15] Borshch V, Shiyankovskii S V, Li B X and Lavrentovich O D 2014 *Phys. Rev. E* **90** 062504
- [16] Lavrentovich O D, Nazarenko V, Sergan V and Durand G 1992 *Phys. Rev. A* **45** R6969
- [17] Li B X, Xiao R L, Paladugu S, Shiyankovskii S V and Lavrentovich O D 2019 *Opt. Express* **27** 3861
- [18] Golovin A B, Shiyankovskii S V and Lavrentovich O D 2003 *Appl. Phys. Lett.* **83** 3864
- [19] Yin Y, Gu M, Golovin A, Shiyankovskii S V and Lavrentovich O D 2004 *Mol. Cryst. Liq. Cryst.* **421** 133
- [20] Dayton D, Browne S, Gonglewski J and Restaino S 2001 *Appl. Opt.* **40** 2345
- [21] Duan W, Chen P, Ge S J, Liang X and Hu W 2019 *Crystals*. **9** 111
- [22] Liu C Y, Yen C F, Hung Y H, Tu C M, Wu G Y and Chen H Y 2021 *J. Mater. Chem. C* **9** 16672
- [23] Hsiao Y C, Yeh E R and Lee W 2017 *Mol. Cryst. Liq. Cryst.* **644** 12
- [24] Suyama S, Date M and Takada H 2000 *Jpn. J. Appl. Phys.* **39** 480
- [25] Song Z, Li Z, Shang X, Li C Y, Ma L L, Lu Y Q and Li B X 2023 *Chin. Opt. Lett.* **21** 010501
- [26] Tang C Y, Huang S M and Lee W 2011 *Dyes Pigm.* **88** 1
- [27] Hsiao Y C and Lee W 2013 *Opt. Express* **21** 23927
- [28] Takikawa Y, Kaneko K, Adachi R, Orihara H and Iwata M 2021 *Jpn. J. Appl. Phys.* **60** 125503
- [29] Gökçen M, Köysal O, Yıldırım M and Altındal Ş 2012 *J. Phys. Chem. Solids* **73** 987
- [30] Kumar A, Silotia P and Biradar A 2011 *Appl. Phys. Lett.* **99** 072902
- [31] Manohar R, Pandey K K, Srivastava A K, Misra A K and Yadav S P 2010 *J. Phys. Chem. Solids* **71** 1311
- [32] Song J K, Manna U, Fukuda A and Vij J K 2007 *Appl. Phys. Lett.* **91** 042907
- [33] Porenta T, Ravnik M and Zumer S 2011 *Soft Matter* **7** 132
- [34] Schadt M 1982 *Mol. Cryst. Liq. Cryst.* **89** 77
- [35] Berry M 1984 *Phys. Bull.* **35** 438